THE
PHYSICAL REVIEW

A journal of experimental and theoretical physics established by E. L. Nichols in 1893

SECOND SERIES, VOL. 148, NO. 2 12 AUGUST 1966

Magnetic Moment Distribution of Nickel Metal*

H. A. MOOK†
Division of Engineering and Applied Physics, Harvard University, and Massachusetts Institute of Technology, Cambridge, Massachusetts
(Received 2 March 1966)

The magnetic form factor of nickel has been determined for the first 27 Bragg reflections by the polarized-neutron-beam technique. Fourier inversion of the form factor shows that the moment density is quite asymmetric about the lattice sites and is negative in the region between the lattice sites. The measured form factor agrees well with a free-atom form factor for Ni^{++} provided a uniform negative contribution is included in the moment density. From the comparison of the free-atom and measured form factors it is found that $81\pm1\%$ of the $3d$ magnetic electrons occupy T_{2g} orbitals, compared with the 60% required for spherical symmetry. The size of the negative contribution needed for agreement between the measured and free-atom form factors agrees well with that given by the Fourier inversion, and the analysis of the data is consistent with the following model for the magnetization of nickel: $3d$ spin$+0.656\mu_B$, $3d$ orbit$+0.055\mu_B$, negative contribution $-0.105\mu_B$.

I. INTRODUCTION

THE angular distribution of the neutron magnetic scattering from a ferromagnet is given by a form factor that is the Fourier transform of the magnetic moment density. Thus, by making a precise measurement of the magnetic scattering the spatial dependence of the periodic magnetic moment can be determined. We have used the polarized neutron beam technique to measure the magnetic form factor of nickel metal.

Despite the fact that a large amount of work has been devoted to understanding the nature of the electronic structure in the transition metals, very little precise knowledge of the magnetic electrons in the ferromagnetic metals is available. Most of the magnetic scattering comes from unpaired $3d$ electron spins. The neutron diffraction measurements give direct information about the spatial distribution of the periodic spin density that is nearly free of theoretical approximations. There is an orbital contribution to the magnetization so some of the magnetic scattering takes place from the orbital moment. However, since the orbital contribution is small, and the orbital and spin form factors are similar in shape, the orbital moment introduces only a small uncertainty in the interpretation of the data. In fact, it is unusual in the study of the transition metals that precise experimental results have such a direct and meaningful interpretation.

Magnetic scattering amplitudes are generally quite small and polarized neutrons must be used for accurate form-factor measurements. The first form-factor measurements using polarized neutrons were made by Nathans, Shull, Shirane, and Andresen[1] on iron and nickel. Although the data on nickel included only eight reflections, with fairly large error brackets, Weiss and and Freeman[2] interpreted the measurements as showing a departure of the $3d$ electrons from spherical symmetry. In a cubic field the degenerate $3d$ orbitals split into triply degenerate T_{2g} orbitals and doubly degenerate E_g orbitals. The T_{2g} orbitals are peaked along the cube body diagonal direction while the E_g orbitals are peaked along the cube edges. Weiss and Freeman suggested that the magnetic electrons were predominantly of T_{2g} symmetry and estimated that 75% of the $3d$ electrons were in T_{2g} orbitals compared to the 60% required for spherical symmetry. The accuracy of the neutron data did not warrant the consideration of an orbital

* This work was supported by grants from the Advanced Research Projects Agency to Harvard University and from the National Science Foundation to Massachusetts Institute of Technology.

† Present address: Solid State Division, Oak Ridge National Laboratory, Oak Ridge, Tennessee.

[1] R. Nathans, C. G. Shull, G. Shirane, and A. Andresen, J. Phys. Chem. Solids **10**, 138 (1959).

[2] R. J. Weiss and A. J. Freeman, J. Phys. Chem. Solids **10**, 147 (1959).

contribution to the form factor or the consideration of scattering from other than $3d$ electrons.

Since the work of Nathans *et al.*, a number of form factor measurements have been reported.[3-7] The most interesting of these to compare with nickel are the very complete measurements of Shull and Yamada[3] for iron and those of Moon[4] for hexagonal cobalt. Shull and Yamada found that the magnetic form factor for iron at a given value of $(\sin\theta)/\lambda$ is dependent on the direction of scattering through the crystal, and thus that the magnetic moment distribution is aspherical about the nucleus. Their analysis of the form factor data showed that 47% of magnetic electrons had T_{2g} symmetry. Moon found that the magnetic form factor for hexagonal cobalt is a smooth function of $(\sin\theta)/\lambda$ so that the moment distribution in hexagonal cobalt is almost spherical.

The data taken by Shull and Yamada, and by Moon are sufficiently extensive that they could obtain Fourier maps for the moment density. These maps show that in both iron and cobalt the magnetic moment density is negative in the region far removed from the lattice sites. It was suggested by Shull and Yamada that the negative density possibly resulted from $4s$ electrons oppositely polarized to the $3d$ electrons.

Two objectives of this work on nickel were to obtain a better picture of the asymmetry of the magnetic electrons, and to see if any negative regions appear in the magnetic moment distribution. The magnetic scattering amplitude of nickel is considerably smaller than the nuclear scattering amplitude so the nickel measurements required more neutron counting time than the iron or cobalt measurements. Nevertheless, we were able to determine the magnetic form factor of nickel for the first 27 Bragg reflections, which is sufficient to give an accurate picture of the magnetic moment distribution.

II. EXPERIMENTAL TECHNIQUE

The experiments were performed on a polarized beam spectrometer installed at the M.I.T. nuclear reactor. The experimental arrangement was similar to that described by Nathans *et al.* The polarized beam technique is used to measure the size of the interference term between the nuclear and magnetic scattering. The magnetic-scattering amplitude can be determined much more accurately from this interference term than from a direct measurement of the magnetic-scattering intensity. The interference term is linear in the scattering amplitudes, and thus the sign of the magnetic-scattering amplitude can also be measured directly. The experiment consists of measuring the intensity in a Bragg peak when the incident neutrons are polarized parallel and then antiparallel to the sample magnetization. For an ideal experiment when no corrections to the data need be made, the ratio of these two intensities is given by

$$R=\left(\frac{1-p/b}{1+p/b}\right)^2, \tag{1}$$

where p and b are, respectively, the magnetic and nuclear scattering amplitudes and R is called the flipping ratio. R is the quantity actually measured in the experiment and p/b is found from (1). Unfortunately, the ideal case is seldom realized in practice and there are corrections to the data that need to be made, particularly for the first few reflections. The data had to be corrected for incomplete neutron polarization, half wavelength contamination in the neutron beam, single crystal extinction effects, and multiple reflections in the sample crystal. The neutron polarization could be measured accurately and was high in all cases. The polarization corrections were thus small and could be applied with certainty. The half-wavelength contamination in the beam was very small and introduced negligible corrections in most cases. Extinction and multiple scattering were considerably more troublesome and deserve some discussion.

A. Extinction

In treating the problem of extinction one usually makes the assumption, first proposed by Darwin,[8] that the sample crystal consists of a large number of small perfect mosaic blocks tipped slightly in angle relative to one another. Secondary extinction results from the reduction in beam strength seen by those blocks deep in the sample relative to those near the surface where the neutron beam enters. All measurements were performed by symmetric transmission of a crystal of uniform thickness. For this case the secondary extinction problem has been solved exactly.[9] The size of the extinction correction depends on the mosaic width, the neutron wavelength, the Bragg angle, and the crystal thickness. Each of these factors was exploited in reducing secondary extinction. The most success was obtained by reducing the crystal thickness. Crystal slices as thin as 0.0038 cm were employed for long counting periods. Measurements from a set of crystal slices of various thicknesses were used to extrapolate the flipping ratio to zero sample thickness. Several sample crystals were examined at wavelengths of 1.05 and 0.77 Å, and many cross checks between different crystals were employed. By controlling the physical characteristics of the crystals and the geometry of the experiment, secondary extinction was reduced to such an extent that corrections could be

[3] C. G. Shull and Y. Yamada, J. Phys. Soc. Japan, **17**, Suppl. BIII, 1, 1962; C. G. Shull, *Electronic Structure and Alloy Chemistry of the Transition Elements* (Interscience Publishers, Inc., New York, 1963), p. 69.
[4] R. Moon, Phys. Rev. **136**, A195 (1964).
[5] S. J. Pickart and R. Nathans, Phys. Rev. **123**, 1163 (1961).
[6] G. Shirane, R. Nathans, and C. W. Chen, Phys. Rev. **134**, A1547 (1964).
[7] W. C. Phillips, Phys. Rev. **138**, A1649 (1965).
[8] C. G. Darwin, Phil. Mag. **43**, 800 (1922).
[9] G. E. Bacon and R. D. Lowde, Acta Cryst. **1**, 303 (1948).

applied with an uncertainty less than the needed accuracy of the data.

Primary extinction is much smaller than secondary extinction and we will only consider it briefly. Primary extinction results from the reduction in neutron intensity seen by those atoms at the bottom of a mosaic block relative to those at the top of the block where the beam enters. Probably the most physically significant formulation of primary extinction is due to Ekstein.[10] Using the Ekstein formulation one can distinguish between primary and secondary extinction by their different dependence on the scattering angle. A careful measurement of the angular dependence of the flipping ratio showed that the error introduced by primary extinction was small compared to the statistical uncertainty of the data.

B. Multiple Scattering

Moon and Shull[11] have shown that multiple reflections have a large effect on the neutron intensity diffracted by single crystals. The effects of multiple reflections cancel somewhat in taking the flipping ratio; nevertheless, the effects are still large enough that they must be correctly taken into account. For this reason all the data were collected as the crystal was rotated slowly in azimuth about the scattering vector. Any abrupt changes in the Bragg-reflected intensity with azimuth angle are an indication of multiple reflections and the data in that region were disregarded. The magnitude of multiple scattering effects is very sensitive to the crystal geometry and very little multiple scattering was seen with thin crystal slices.

III. DISCUSSION OF RESULTS

The most direct method of analyzing the scattering data is to Fourier transform the measured form factor to obtain density maps of the magnetic moment distribution. The magnetic scattering amplitude for the (000) reflection cannot be measured but can be calculated from the magnetization. If we take the magnetization of nickel to be $0.606\mu_B$ per atom at 0°K and the relative magnetization at room temperature to be 0.946 of that at 0°K,[12] the magnetic scattering amplitude for the (000) reflection at room temperature is given by

$$p(000)=(\gamma e^2/mc^2)(\tfrac{1}{2}\langle n_B\rangle)=0.155\times10^{-12}\text{ cm}, \quad (2)$$

where $\langle n_B\rangle$ is the room temperature number of Bohr magnetons per atom and γ is the magnetic moment of the neutron in nuclear magnetons. To find the magnetic scattering amplitude from the measured data we must know the nuclear scattering amplitude. $1.03\pm0.01\times10^{-12}$ cm is the accepted value of the nuclear scattering amplitude of nickel.[13] The form factor is given by the magnetic scattering amplitude normalized to unity at (000). The results of the polarized beam experiments are given in Table I. A 1% error in the normalization of the form factor has been included to take account of the uncertainty in our knowledge of the nuclear scattering amplitude.

TABLE I. Summary of experimental data.

hkl	$(\sin\theta)/\lambda$ (Å^{-1})	p/b	f
111	0.2462	0.1193±0.0006	0.793±0.009
200	0.2843	0.1058±0.0006	0.703±0.008
220	0.4021	0.0672±0.0005	0.447±0.005
311	0.4715	0.0483±0.0005	0.321±0.005
222	0.4925	0.0468±0.0004	0.311±0.004
400	0.5687	0.0236±0.0004	0.157±0.003
331	0.6197	0.0253±0.0004	0.168±0.003
420	0.6358	0.0198±0.0004	0.132±0.003
422	0.6965	0.0162±0.0005	0.108±0.004
511	0.7387	0.0054±0.0005	0.036±0.004
333	0.7387	0.0165±0.0004	0.109±0.003
440	0.8042	0.0087±0.0005	0.058±0.004
531	0.8411	0.0048±0.0005	0.032±0.004
600	0.8530	−0.0037±0.0004	−0.025±0.003
442	0.8530	0.0079±0.0005	0.052±0.004
620	0.8991	−0.0014±0.0005	−0.009±0.004
533	0.9322	0.0054±0.0005	0.036±0.004
622	0.9430	0.0009±0.0005	0.006±0.004
444	0.9850	0.0056±0.0005	0.037±0.004
551	1.0153	0.0014±0.0005	0.009±0.004
711	1.0153	−0.0071±0.0005	−0.047±0.004
640	1.0252	−0.0001±0.0005	−0.001±0.004
642	1.0639	0.0001±0.0005	0.001±0.004
731	1.0920	−0.0040±0.0005	−0.027±0.004
553	1.0920	0.0018±0.0005	0.012±0.004
800	1.1373	−0.0095±0.0005	−0.063±0.004
733	1.1637	−0.0025±0.0005	−0.017±0.004

The periodic magnetic moment density in Bohr magnetons per cubic angstrom is given by

$$\rho(r)=(\langle n_B\rangle/V)\sum_{hkl}F_{hkl}e^{-i\mathbf{k}\cdot\mathbf{r}}, \quad (3)$$

where V is the unit cell volume and

$$F_{hkl}=\sum_j f_{hkl}e^{i\mathbf{k}\cdot\mathbf{r}_j}, \quad (4)$$

where the summation is to be taken over all the atomic positions of the unit cell and f_{hkl} is the form factor. The Fourier summation was done on the M.I.T. Computation Center 7094 computer. Figure 1 shows the magnetic moment density plotted along the three main crystallographic directions. We see there is considerable asymmetry in the moment distribution as $\rho(r)$ is spread out along the [111] direction relative to the [100] direction. This shows that the magnetic electrons are predominantly in T_{2g} orbitals. The density $\rho(r)$ falls to zero quite rapidly and is quite small over most of the unit cell.

The density seen in Fig. 1 is really the true density as seen with finite resolution since data are available only up to the 733 reflection at $(\sin\theta)/\lambda=1.16$ Å^{-1}. This is the optical equivalent of viewing an object through a finite-sized aperture. The resolution function in Fig. 1 is

[10] H. Ekstein, Phys. Rev. **83**, 721 (1951).
[11] R. M. Moon and C. G. Shull, Acta Cryst. **17**, 805 (1964).
[12] P. Weiss, quoted in Bozarth, *Ferromagnetism* (D. Van Nostrand, Inc., New York, 1951), p. 270.
[13] G. E. Bacon, *Neutron Diffraction* (Oxford University Press, London, 1955), p. 28.

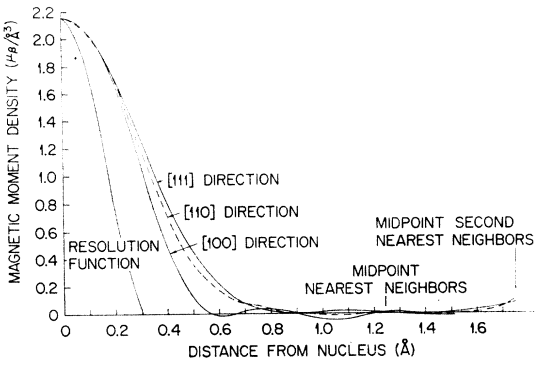

FIG. 1. Distribution of magnetic moment density along the three major crystallographic directions.

obtained by Fourier transforming a constant form factor for all reflections up to and including (733) and letting the form factor be zero for all higher reflections. The resolution function shows the diffraction effects that would be produced in attempting to map a lattice of points using the same set of reflections used in the nickel measurements. Any detail finer than the width at half-maximum of the resolution function cannot be resolved.

The limited resolution also causes the $\rho(r)$ obtained from the Fourier series to oscillate at large r. We would like to be able to determine the size of the moment density in the region between the atoms, but oscillations obscure the real value of $\rho(r)$ which is smaller than the amplitude of the oscillations. The problem is that the Fourier series for $\rho(r)$ converges too slowly to give the moment density in the region between the atoms. This problem has been solved by deriving the Fourier series that gives $\rho(r)$ averaged in space over a small cubic block. The Fourier series for the average density $\bar{\rho}(r)$ is given by

$$\bar{\rho}(r)=\frac{\langle n_\beta\rangle}{V}\int_{x-\delta}^{x+\delta}\int_{y-\delta}^{y+\delta}\int_{z-\delta}^{z+\delta}\sum_{hkl}F_{(hkl)}e^{-2\pi i(hx/a+ky/a+lz/a)}dxdydz$$

$$=\frac{\langle n_\beta\rangle}{V}\frac{1}{(2\pi\delta/a)^3}\sum_{hkl}\frac{F_{(hkl)}}{hkl}\sin\left(\frac{2\pi h\delta}{a}\right)\sin\left(\frac{2\pi k\delta}{a}\right)\sin\left(\frac{2\pi l\delta}{a}\right)e^{-2\pi i(hx/a+ky/a+lz/a)}, \tag{5}$$

where a is the lattice constant and $(2\delta/a)$ is the length of a side of the cubic block over which the average is taken.[14] This series smears out the moment density somewhat but converges much more rapidly than the series given in Eq. (3) because of the factor $(hkl)^{-1}$. The convergence for the point $(a/2,0,0)$ is shown in Fig. 2 for $\delta/a=0.075$. The continued sum of the Fourier series is plotted versus $(\sin\theta)/\lambda$ so successive points are obtained by increasing the number of terms in the series by one, except the average is shown when two reflections fall at the same value of $(\sin\theta)/\lambda$. The size of the oscillations is a measure of the convergence of the series. The $\rho(r)$ given by Eq. (3) is still oscillating widely at $(\sin\theta)/\lambda=1.16$ Å^{-1}, but the series for $\bar{\rho}(r)$ has converged nicely to $-0.0085\mu_B$/Å^3. Several different cube sizes $(2\delta/a)^3$ were tried. Good convergence has been obtained with cube blocks as small as 0.07 lattice constants on a side. For much smaller blocks, $\bar{\rho}(r)$ does not converge well and would approach the $\rho(r)$ given by Eq. (3) if the cube became small enough. If the block is large the moment in the region of the atom is smeared out over the entire unit cell. For intermediate block sizes the Fourier series for $\bar{\rho}(r)$ converges to a negative density of about $0.0085\mu_B$/Å^3 in the regions of the unit cell farthest removed from the lattice sites.

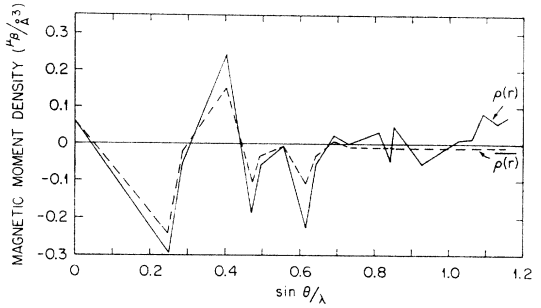

FIG. 2. Fourier series convergence at the point (a/2,0,0) for $\rho(r)$ the magnetic moment density and for $\bar{\rho}(r)$ the magnetic moment density averaged over a cubic block 0.15 lattice constants on a side. The total experimental error gives an uncertainty in $\bar{\rho}(r)$ of less than 0.004 μ_B/Å^3.

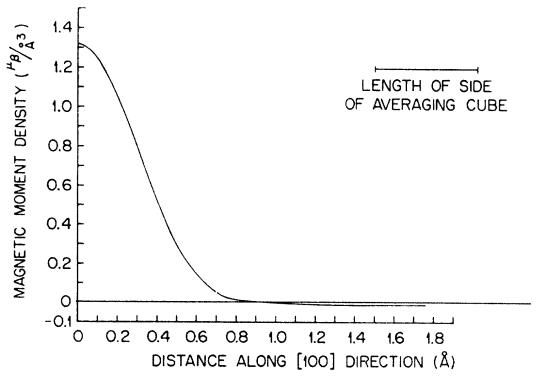

FIG. 3. The average magnetic moment density $\bar{\rho}(r)$ for a cubic block 0.15 lattice constants on a side plotted along the [100] direction.

[14] This series giving the average density is an extension to the three dimensional case of the series used by Moon to obtain the average projected moment density.

$\bar{\rho}(r)$ for a cubic block 0.150 lattice constants on a side is plotted in Fig. 3 for the direction along the [100] axis. Note that the moment density hump near the origin is spread out more than in Fig. 1 and the maximum value of the moment density is thus reduced. The $\bar{\rho}(r)$ for other directions in the crystal are similar to $\bar{\rho}(r)$ along [100], the part of the density in the $3d$ hump being slightly different in different directions owing to the asymmetry in the moment distribution. The negative background seems to be fairly constant over a large part of the unit cell. Of course any variations smaller than the averaging block size would be obscured by the averaging process.

The magnetic moment density in the [100] and [110] planes is shown on the contour maps in Figs. 4 and 5. These maps again emphasize the strong asymmetry in the magnetic electron distribution. The part of the moment density near the atomic sites in the $3d$ magnetic moment humps was given by the series for $\rho(r)$. The series for $\bar{\rho}(r)$ was employed to give the moment density in the region far removed from the lattice sites. The Fourier maps show that the moment density consists of large positive asymmetric contributions near the lattice sites imposed on a small negative background. It is worthwhile to emphasize that the Fourier inversion technique requires no theoretical model of the magnetic moment distribution and gives the spatial distribution of the magnetic moment density directly from the measured data and the calculated point at [000].

IV. COMPARISON OF MEASURED AND CALCULATED FORM FACTORS

A second approach to analyzing the scattering data is to compare the measured form factor with any calculated form factors that are available. With the exception of some recent work by Hodges, Lang, Ehrenreich, and Freeman,[15] theoretical calculations giving form factors for nickel atoms in a metal lattice have not been available. However, Hartree-Fock free-atom form factors for nickel are available for various stages of ionization and the measured form factor was compared with the free-atom form factors. Three contributions were considered in constructing the free-atom form factor: an electron-spin contribution, an orbital contribution, and a contribution from the spin-polarization effects of the core electrons inside the $3d$ shell. The form factor thus may be written as

$$f(\mathbf{k})=(2/g)f_{\text{spin}}(\mathbf{k})+[(g-2)/g]f_{\text{orbit}}(\mathbf{k})+f_{\text{core}}(\mathbf{k}), \quad (6)$$

where g is the spectroscopic splitting factor. For nickel, $g=2.20$ as given by the magnetomechanical measurements of Scott.[16] The spin contribution is by far the largest, the orbital contribution being about 10% and the core contribution being almost negligible. When the measured form factor is compared with free-atom form factors calculated using Eq. (6), it is found that the measured form factor is appreciably higher than the calculated form factors. However, the Fourier maps show that there is a negative contribution to the moment density; thus it would be reasonable to include this negative contribution in the comparison between the measured and free-atom form factors. We can do this by assuming that the spin part of the form factor can be written in the following manner:

$$f_{\text{spin}}(\mathbf{k})=(1+\alpha)f_{3d}(\mathbf{k})-\alpha\delta(\mathbf{k}), \quad (7)$$

where α is a constant. $\alpha\delta(k)$ only makes a contribution at $k=0$ and thus corresponds to a uniform contribution to the magnetization. This treatment of the spin part of the form factor is the same as that used by Moon.[4] As he points out, the proper way to ask whether the shape of the observed periodic spin density is the same as that given by a superposition of $3d$ atomic functions is to test for proportionality between the observed and calculated form factors for all reflections other than

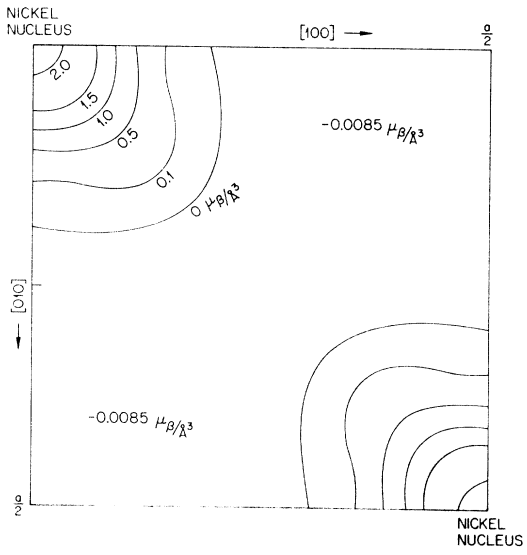

FIG. 4. The magnetic moment distribution in the [100] plane.

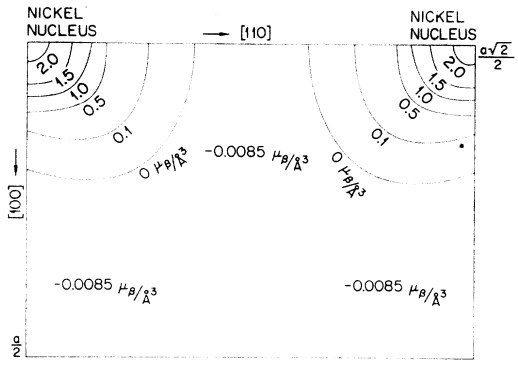

FIG. 5. The magnetic moment distribution in the [110] plane.

[15] L. Hodges, N. D. Lang, H. Ehrenreich, and A. J. Freeman, J. Appl. Phys. 37, 1449 (1966).
[16] G. G. Scott, J. Phys. Soc. Japan, 17, Suppl. B1, 372, 1962.

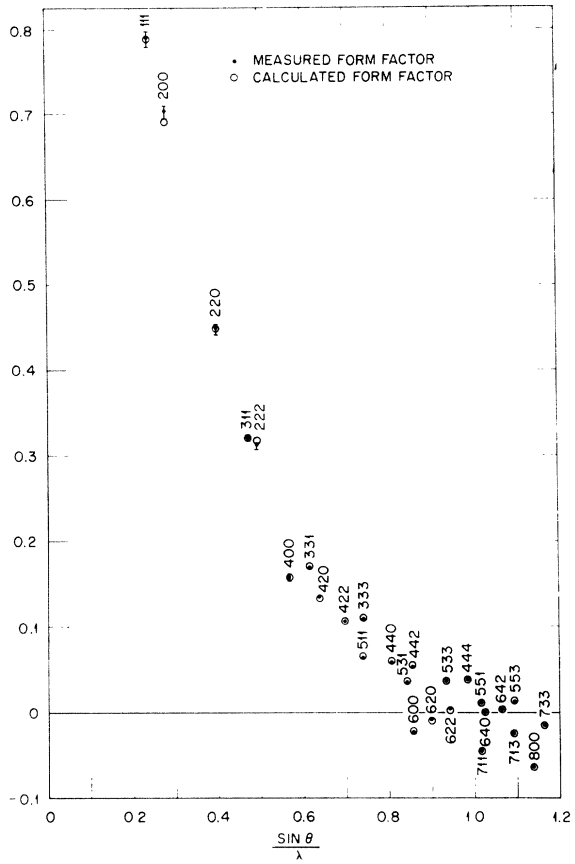

FIG. 6. Comparison of calculated and measured form factors.

(000). The introduction of the delta function permits us to compare the shape of the radial distribution of the moment density in nickel metal with that in a free atom and still deal with normalized form factors.

Because of the asymmetry of the magnetic electrons the form factor of nickel is not a smooth function of $(\sin\theta)/\lambda$. In a cubic field the fivefold degenerate orbitals of the $3d$ electrons split into triply degenerate T_{2g} orbitals which transform like xy, xz, and yz; and doubly degenerate E_g orbitals which transform like $3z^3-r^2$ and x^2-y^2. The scattering amplitudes for these two sets of orbitals are different, and Weiss and Freeman[2] have shown that the spin part of the form factor for $3d$ electrons in a cubic field can be written

$$f_{3d}(\mathbf{k})=\langle j_0\rangle+(\tfrac{5}{2}\gamma-1)A_{hkl}\langle j_4\rangle, \qquad (8)$$

where $\langle j_0\rangle$ represents the spherical part of the spin distribution and $\langle j_4\rangle$ the aspherical part. γ is the percentage of $3d$ electrons in E_g orbitals and is 40% for spherical symmetry. A_{hkl} is a function of the direction that is being examined in the crystal and is given by

$$A_{hkl}=\frac{h^4+k^4+l^4-3(h^2k^2+h^2l^2+k^2l^2)}{(h^2+k^2+l^2)^2}. \qquad (9)$$

The aspherical orbital contribution is small compared to the aspherical spin contribution and we will neglect it. The form factor then becomes

$$f(\mathbf{k})=(2/g)(1+\alpha)[\langle j_0\rangle+(\tfrac{5}{2}\gamma-1)A_{hkl}\langle j_4\rangle]+[(g-2)/g]f_{\text{orb.}}(\mathbf{k})+f_{\text{core}}(\mathbf{k})-(2/g)\alpha\delta(\mathbf{k}). \qquad (10)$$

Watson and Freeman have performed several different calculations for the spin and orbital parts of the form factor corresponding to different electron configurations. The spin parts of the calculations have been published[17–20] and the orbital parts were privately communicated. The core part of the form factor was obtained from an unrestricted Hartree-Fock calculation for Ni^{++}.[19] The data were compared with all the available calculations and the best fit was obtained using the $\langle j_0\rangle$ from an unrestricted calculation for Ni^{++},[19] the $\langle j_4\rangle$ for Ni^{++},[17] the orbital contribution for Ni^{++}, and setting $\gamma=19\%$ and $\alpha=0.19$. The comparison of the measured and calculated form factors is shown in Fig. 6. Note that the agreement is extraordinarily good and thus that the shape of the moment distribution in metallic nickel is almost identical to the shape of a moment distribution which consists of free atom-like distributions imposed on a constant negative background.

$\langle j_0\rangle$ is not needed to find γ, since $\langle j_0\rangle$ can be eliminated between two equations like (10) written for the same value of $(\sin\theta)/\lambda$ but for different hkl. In practice the best way to determine γ is to Fourier transform the difference between the calculated and measured results for various γ. For the correct value of γ the Fourier transform of the difference will have spherical symmetry. In this manner it was determined that the best fit is obtained if $81\pm1\%$ of the $3d$ magnetic electrons are placed in T_{2g} orbitals.

Setting $\alpha=0.19$ corresponds to including a uniform negative contribution to the moment density of $-0.0091\mu_B/\text{Å}^3$. This agrees well with the negative moment density observed on the Fourier maps. The two methods of analyzing the data are thus consistent with each other and lead to a model of the magnetization which distributes the magnetic moment per atom in the following way:

$3d$ spin $0.656\mu_B$,

$3d$ orbit $0.055\mu_B$,

Negative contribution $-0.105\mu_B$.

If the negative contribution were spaced uniformly throughout the unit cell it would amount to a magnetization field of about 1.1 kG.

We cannot determine the origin of the negative contribution from the neutron diffraction measurements. However, one very good possibility is that the negative

[17] R. E. Watson and A. J. Freeman, Acta Cryst. **14**, 27 (1961).
[18] See Ref. 17, p. 231.
[19] R. E. Watson and A. J. Freeman, Phys. Rev. **120**, 1125 (1960).
[20] See Ref. 19, p. 1134.

moment density arises from $4s$ electrons whose spin is oppositely polarized from the $3d$ electrons. This possibility was utilized by Shull and Yamada in the analysis of their form-factor data for iron. $4s$ form factors fall to immeasurably small values before the first Bragg reflection. Equation (10) can thus be taken to represent scattering from both $3d$ and $4s$ electrons if $3d$, $4s$ cross terms are neglected. It is difficult to determine the nature of any $3d$, $4s$ cross terms that would be present; however it is expected that any such terms would be very small.

It is also plausible that the negative contribution stems from spin polarization effects in the $3d$ band. It is expected that the wave functions at the top of the $3d$ band are very similar to free-atom wave functions.[21,22] Presumably this is why the $3d$ free-atom form factor provides the good fit to the data shown in Fig. 6. The $3d$ wave functions at the bottom of the band are quite diffuse. There is no net difference in the number of electrons with spin up and down at the bottom of the band, however scattering can still take place from the bottom of the band if there is a difference in the radial distribution of spin-up and spin-down electrons. Watson and Freeman's unrestricted Hartree-Fock calculation for Ni^{++} shows that there is some variation in the radial wave functions for spin-up and spin-down electrons in the free atom. Perhaps in a metal these spin polarization effects can account for the negative density observed on the Fourier maps. In this case all the scattering would come from the $3d$ band and it would be unnecessary to include $4s$ electron effects.

It is conceivable that expression (2) for $p(000)$ is incorrect in a metal and that there is no negative contribution to the moment density. This seems unlikely as the magnetic cross-section expressions from which (2) is derived appear to give the correct experimental results for the magnetic scattering from salts and generally seem valid for the rare-earth metals. Moreover, if the magnetic scattering amplitude expression (2) were incorrect, one should expect to find that the relative negative contribution in iron, cobalt, and nickel is the same, whereas these are not the same, the negative contribution being 18% for cobalt and 10% for iron.

V. SUMMARY

The magnetic form factor of nickel has been determined for the first 27 Bragg reflections. The form factor contains information about the spatial distribution of the magnetic moment density in the unit cell. There are two approaches one can take in obtaining this information. The first is to Fourier transform the form factor to obtain a three dimensional map of the moment distribution. The Fourier series gives accurate information about the shape of the moment density in the regions of the unit cell where the moment density is large but converges too slowly to give any information in the region far from the lattice sites where the moment density is small. A Fourier series was devised that gives the density averaged in space over a cubic block. This series smears out the moment distribution somewhat but converges quickly, giving accurate information in the region where the moment density is small. A map of the moment density derived from these Fourier series shows that the magnetic electrons must be predominantly in T_{2g} orbitals and pictures the moment distribution as being similar to asymmetric free atom distributions placed on a negative background.

The second approach to analyzing the data is to compare the measured form factor with calculated form factors. Unfortunately, there are no calculated form factors available for nickel metal; however a number of free-atom form factors are available for several stages of ionization. It is surprising to find that the free atom form factor for Ni^{++} fits the data extremely well provided a uniform negative contribution is added to the moment density. The measured form factor is not a smooth function of $(\sin\theta)/\lambda$ and from the comparison with the free-atom form factor we find that $81\pm1\%$ of $3d$ electrons occupy T_{2g} orbitals. The size of the negative contribution needed for agreement between the calculated and measured form factors agrees well with that observed in the Fourier maps, and the two approaches to analyzing the data appear to be consistent with each other in every way.

This work on nickel completes the magnetic form-factor measurements for the three classical ferromagnets. The relative size of the negative contribution to the moment density of nickel is considerably larger than that observed for iron but similar to that found for cobalt. Nickel has considerably more asymmetry in its moment distribution than iron or cobalt, iron having 47% of its magnetic electrons in T_{2g} orbitals and cobalt having an almost spherical moment distribution.

ACKNOWLEDGMENTS

It is a pleasure to acknowledge the help and guidance of Professor C. G. Shull and Professor R. V. Jones in all phases of this research.

Dr. A. J. Freeman provided the free-atom calculations and was the source of many helpful suggestions.

The author has profited by discussions with Professor H. Ehrenreich, Dr. R. J. Weiss, and the following members of the M.I.T. neutron diffraction group: Dr. Walter Phillips, Dr. Alan Wedgwood, Dr. Stephen Spooner, Yuji Ito, and Armand D'Addario.

[21] J. H. Wood, Phys. Rev. **117**, 714 (1960).
[22] F. Stern, Phys. Rev. **116**, 1399 (1959).